

# The Aluminization of Platinum and Platinum-Coated IN-738

M. R. JACKSON AND J. R. RAIRDEN

The chemistry and morphology of aluminide coatings formed on platinum and platinum-coated IN-738 have been studied. Most of the aluminide coatings evaluated were applied using the pack cementation process. For aluminized platinum a series of intermetallic Pt-Al compounds form. The stoichiometries of these compounds are essentially in agreement with those that would be predicted based upon phase diagram considerations. For aluminized, platinum-coated IN-738, the coating morphology and chemistry are highly dependent upon the thickness of the platinum layer. A relatively thick platinum layer (~25 microns) confines the initial reaction for the aluminizing conditions used so that refractory metal elements from the substrate are excluded from the outer regions of the coating. Thinner platinum layers only partially confine the reaction and do not exclude the refractory metals from the coating. Microstructures that develop are related to the appropriate phase diagrams.

THE environment which exists in the hot-gas portion of industrial gas turbines is extremely aggressive.<sup>1</sup> Temperatures in the range of 900°C are sufficient to cause accelerated oxidation/hot corrosion attack of Ni-base superalloy turbine components by the fuel and atmospheric constituents, such as sulfates, chlorides, vanadates and sodium and lead ions. To increase the useful service life for superalloy components, there is a continuing need for improved hot-corrosion resistant coatings. Diffusion aluminide and CoCrAlY overlay coatings have proven useful in turbine environments.<sup>1,2</sup>

Another coating system for nickel-base superalloys has been described by Lehnert and Meinhardt.<sup>3-6</sup> This system is reported to give a 230 pct improvement in hot-corrosion resistance over simple aluminide coatings. The platinum-aluminide coating system is applied by first electrolytically depositing a platinum layer less than 10  $\mu\text{m}$  thick, then pack aluminizing the substrate to form a platinum-aluminide-type coating. Aluminizing processes have been reviewed extensively elsewhere.<sup>7-10</sup> The degradation process for aluminide coatings involves loss of aluminum in two directions; (1) outward loss by oxide formation and spallation, and (2) inward loss by interdiffusion with the substrate. The Pt-Al coating was developed during a search for a "diffusion barrier" to prevent or retard the migration of aluminum from the coating into the substrate. However, the compositional profile found by Lehnert and Meinhardt<sup>3</sup> indicated that, after aluminization, the platinum remained concentrated in the outermost region of the duplex coating and was not a diffusion barrier.

The goal of this study was to gain an understanding of the effects of an initial platinum layer on the formation of aluminide coatings on IN-738.\* The aluminiza-

\*59.6 a/o Ni, 8.2 Co, 17.5 Cr, 7.2 Al, 4.0 Ti, 1.0 Mo, 0.8 W, 0.5 Nb, 0.6 Ta, 0.03 Zr, 0.6 C.

tion of platinum was studied to provide supplemental data. The pack aluminization of IN-738 has been treated

in detail previously.<sup>10</sup> Aluminum was observed to deposit very rapidly initially, with deposition slowing to a much lower rate soon after the aluminizing pack reaches the aluminizing temperature. Further exposure is primarily a solid-state diffusion anneal. The phases formed during the entire pack process are substantially those predicted from ternary phase diagrams. The manner in which the sequence of events is altered by the presence of a Pt layer on IN-738 can be understood in a similar fashion, and is the subject of this study.

## EXPERIMENTAL TECHNIQUES

The IN-738 substrates were pins cast to 0.47 cm diameter and centerless ground to 0.43 cm diameter. The platinum substrates were cut from 0.1 cm thick sheet or 0.1 cm diameter wire. Platinum layers were deposited on the IN-738 substrates, using the rf sputtering technique. By holding the substrates in a fixed position under the sputtering source during processing, a coating was deposited that varied in thickness from 0 to 25  $\mu\text{m}$  on a single specimen. The pin surface facing the cathode had a coating layer of the maximum thickness, and the surface away from the cathode was uncoated. Between these extremes, the coating had a continuous and gradual variation in thickness. The sputtering system used was a Perkin-Elmer Randex Model 2400. The deposition conditions were ~6 h at 500 watts in  $18 \times 10^{-3}$  torr argon.

The vacuum evaporated Al layers were deposited on rotating wire substrates by the use of a pure (99.99 pct) aluminum source heated by a focused electron beam. A layer 25  $\mu\text{m}$  thick was deposited in 8 min, using a power of 5.5 KW.

The pack aluminizing experiments were done with a 31 cm<sup>3</sup> retort with a snug fitting lid, both made of Inconel 600. The packs were mixtures of Al (Metco 54) and Al<sub>2</sub>O<sub>3</sub> (Linde A-10) powders. The Al powder was preactivated with an aqueous solution of either HF or NH<sub>4</sub>F as described previously.<sup>10</sup> A 20 g charge of powder was used for each pack deposition experiment. Half of the powder was spread in the retort; the substrates, which were cleaned by washing in acetone and rinsing with alcohol, were placed on the

M. R. JACKSON and J. R. RAIRDEN are Metallurgists with General Electric Company, Corporate Research and Development, Schenectady, NY 12345.

Manuscript submitted October 20, 1975.

powder. The remaining powder was spread over the substrates.

The argon atmosphere furnace used for aluminizing was preheated to 1060°C. The retort was placed in the cool zone of the furnace for 2 min and then was pushed into the hot zone. Zero hour as used in this report was the time at which the pack reached the run temperature; this was approximately 12 min after entering the furnace hot zone. At the end of the run, the retort was returned to the cool zone of the furnace until the pack was below 250°C. Conventional metallographic and electron microprobe techniques were used to study microstructures.

## RESULTS AND DISCUSSION

The aluminization of bulk IN-738 and bulk platinum will be discussed first as a basis for understanding the aluminization of Pt coated IN-738.

### A. Aluminization of Bulk IN-738

Earlier studies have described the mechanism of the pack aluminization of superalloys in terms of pack activity.<sup>7-9,11</sup> Microstructures formed in high activity packs resulted from primarily inward diffusion of aluminum, while microstructures formed in low activity packs resulted from primarily outward diffusion of nickel. These conclusions were based on analyses of microstructures formed during several hours of processing. The location of carbide particles, either throughout the coating layer or at the coating/substrate interface, was considered to be evidence supporting these conclusions, since the carbides were presumed to be inert diffusion markers.

A recent study by the present authors has considered microstructural development during aluminization of superalloys from times of a few seconds through times conventionally used in commercial aluminization processes.<sup>10</sup> Aluminization by pack processes and by heat treatment of Al/superalloy couples was discussed and analyzed. For both methods microstructural development included a period when the nominally "inert" carbides were distributed throughout the coating layer and a later period when the carbides were located at the coating/substrate interface. The structural development included those identical with high activity and with low activity pack microstructures. The phases present in the coatings were correlated with the phase diagram for the Ni-Cr-Al system. One of the conclusions of the study was that not only is pack composition a determining factor in microstructural development, but time and temperature of processing control the microstructure for a given pack composition. Furthermore, essentially all pack compositions follow the same sequence of microstructural development for a given processing time and temperature, with pack composition determining the rate of progression through that sequence of development.

In this paper, a brief review of the aluminization of IN-738<sup>10</sup> will serve as an introduction to the present studies. When packs were placed in a 1060°C furnace, samples reached temperature in about 12 min. In that time, two-thirds of the Al that would reach the samples in three hours of aluminizing had already been

deposited. The following model explains the microstructures and chemical profiles that result when substantial amounts of Al are deposited in a few minutes' time. The observed phase growth requires a diffusion coefficient of  $\sim 10^{-5}$  cm<sup>2</sup>/sec., and this value is not consistent with solid state diffusion coefficients for the various phases present.<sup>12</sup> This indicates the probability of liquid phase formation on the substrate surface while Al is being deposited most rapidly. The liquid has a higher solubility for Ni and Al than for Cr, resulting in a region of high Cr (and refractory metals) in the solid at the liquid/solid interface. The liquid subsequently dissolves enough of the substrate to reach a composition that is solid at the processing temperature. Solidification is complete at approximately zero hour; that is, when the sample reaches 1060°C. The remainder of the pack aluminizing process is primarily a diffusion heat treatment. The process can be described in terms of diffusion paths in the Ni-Al-Cr ternary phase diagram. Liquid retention was not accomplished in pack processing because of the delays inherent in quenching samples from an enclosed aluminization pack. However, structures formed on quenched Al/substrate heat treated short-time simulations appear to be quenched from the liquid state.

### B. Aluminization of Bulk Platinum

If the deposition of Al on Ni-base superalloys from an activated pack involves a liquid phase reaction, it might be supposed that the same would be true for deposition of Al on Pt. The solubility of Pt in an Al-rich liquid increases with increasing temperature<sup>13</sup> in much the same manner as the solubility of Ni and Cr in an Al-rich liquid.<sup>14</sup> To study the aluminization of platinum, weight change measurements were made on Pt samples aluminized for several time periods at 1060°C. Fig. 1 compares the aluminization of Pt and of IN-738 for a pack containing 5.8 pct Al, 94 pct Al<sub>2</sub>O<sub>3</sub>, and 0.2 pct NH<sub>4</sub>F. The aluminization of both Pt and IN-738 is characterized by an initial very rapid deposition of Al. This is in accord with results pre-

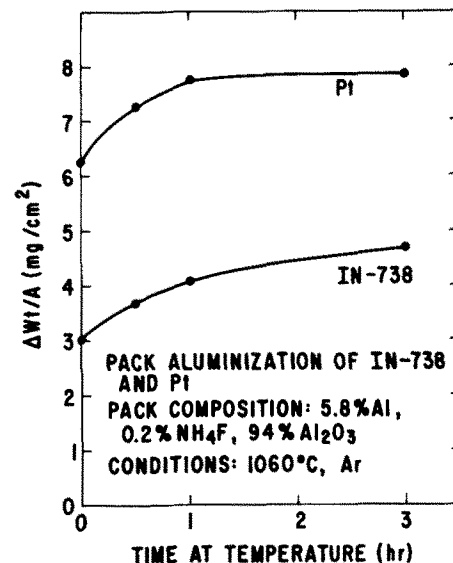


Fig. 1—Change in weight with time of pack aluminization for Pt and IN-738 at 1060°C in an activated 5.8 pct Al pack.

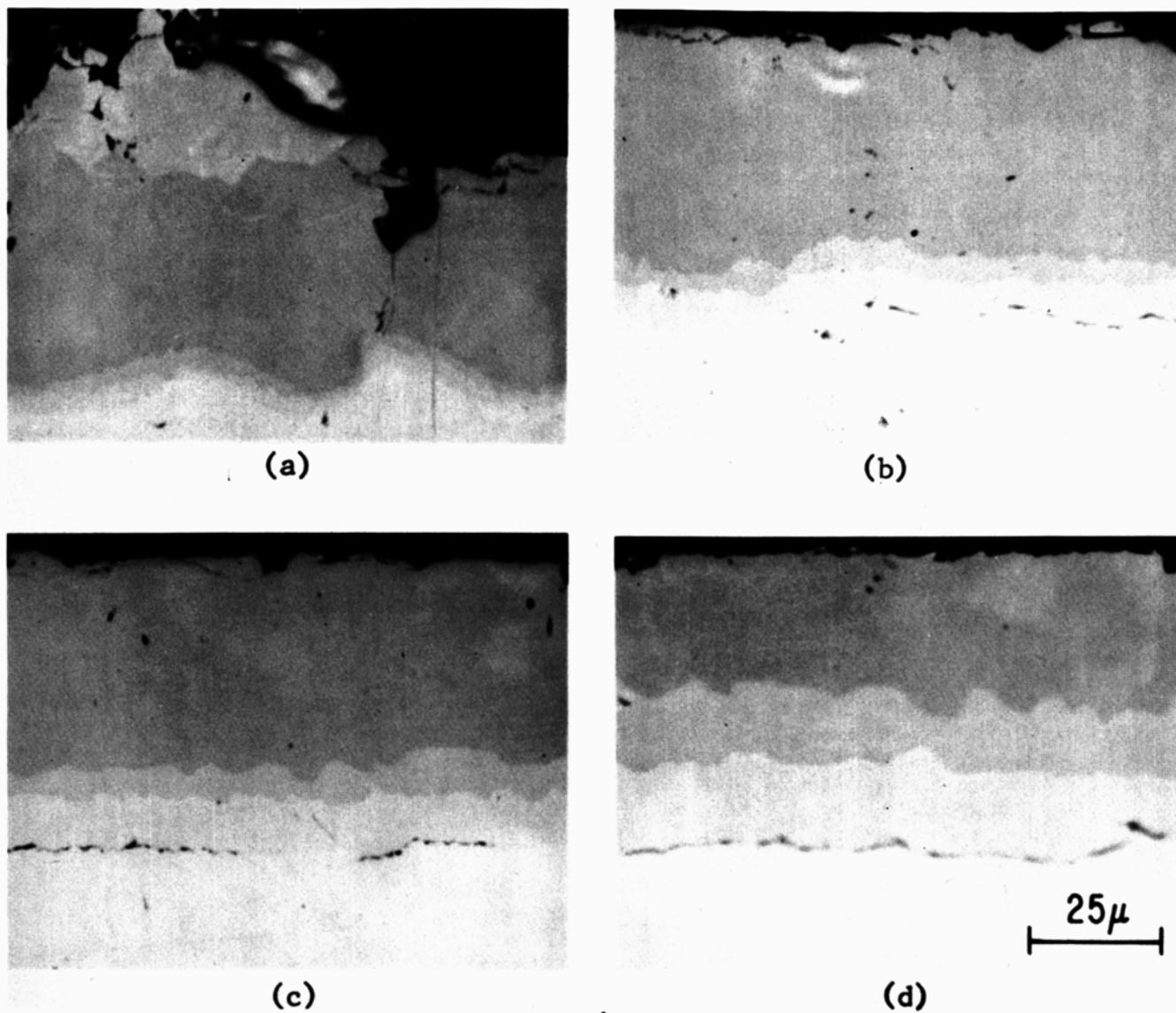


Fig. 2—Microstructures for platinum aluminized at 1060°C in a pack containing 5.8 pct Al, 0.2 pct  $\text{NH}_4\text{F}$ . (a) 0 h, sintered particle region, (b) 1/2 h, (c) 1 h, and (d) 3 h.

viously reported for Ni-base superalloys.<sup>10</sup> Of particular note is the fact that almost twice as much Al is deposited on Pt as on IN-738. This indicates that the rate limiting step in the aluminization of IN-738 using these processing conditions is the assimilation of Al into the substrate rather than the transfer of Al from the pack. Aluminum deposition will cease whenever its activity on the substrate surface is equal to the activity in the vapor. By this reasoning, Pt has a greater capacity than IN-738 for aluminum assimilation.

The large weight gains noted for aluminization of Pt suggest a sequence of liquid formation, substrate dissolution, and subsequent liquid solidification, similar to that proposed for aluminization of superalloys.<sup>10</sup> Metallographic cross sections of aluminized Pt samples are shown in Fig. 2. The compositional profiles of the 0 h, 1/2 h, and 3 h samples were measured by the electron microprobe technique. The compositions of the coating layers for these samples are summarized in Table I. No single aluminizing operation produced all of these phases. For  $\text{PtAl}_4$  to be observed, samples

were treated at 660°C rather than 1060°C. The phase would not be seen in 1060°C treatments because that composition is molten at 1060°C.

All but one of the phases shown in the binary Pt-Al phase diagram<sup>13</sup> were observed for at least one aluminizing temperature. One phase,  $\text{Pt}_3\text{Al}_2$  or  $\text{Pt}_5\text{Al}_3$ , was absent. From the microprobe data and the layer thicknesses, it is difficult to determine which phase is present. The difference in Pt concentration is only 0.8 wt pct between  $\text{Pt}_5\text{Al}_3$  and  $\text{Pt}_3\text{Al}_2$ . It can be seen in Table I that the microanalysis for Pt and Al sums to only 97.6 wt pct and that normalizing the values to 100 pct results in a composition intermediate between  $\text{Pt}_3\text{Al}_2$  and  $\text{Pt}_5\text{Al}_3$ . It is probable that  $\text{Pt}_3\text{Al}_2$  does not exist, since there is little other evidence of its existence.<sup>13</sup> Chatterji, DeVries, and Fleischer<sup>14</sup> have studied the Pt-Al system in detail recently, and observed neither  $\text{Pt}_3\text{Al}_2$  nor  $\text{Pt}_5\text{Al}_3$ , but rather  $\text{Pt}_2\text{Al}$ . The thicknesses of layers observed for aluminizing Pt at 1060°C are summarized in Table II.

For 1060°C processing, the Al-rich liquid should completely solidify when the  $\text{PtAl}_3$  composition [melt-

ing point = 1121°C<sup>13</sup>] is reached. Thereafter, aluminum movement should be by solid-state diffusion. Except for the particle sintered region where aluminum particles were initially in contact with the surface, resulting in a relatively Al-rich layer at 0 h [Fig. 2(a)], there was no PtAl<sub>3</sub> or PtAl<sub>2</sub> remaining in the 0 h samples. This suggests that Al diffusion is quite rapid through the compounds rich in Al, such as PtAl<sub>3</sub>, PtAl<sub>2</sub>, and Pt<sub>2</sub>Al<sub>3</sub>. The more rapid assimilation of Al into Pt than into IN-738 probably is due to: 1) the apparent fast diffusion rate of Al into Pt and (Pt, Al) compounds, and 2) the high atom fraction of Al in PtAl<sub>3</sub> as compared with Ni<sub>2</sub>Al<sub>3</sub> or NiAl.

To test the hypothesis of a liquid phase reaction, a 0.1 cm diameter Pt wire substrate was coated with a 25 μm thick layer of Al, by vacuum deposition, so there was no substrate-coating reaction. A sample of this Al-coated Pt was heat treated for 2 min at 900°C in argon and was examined metallographically. (The phase PtAl<sub>4</sub> exists below 800°C, while the other Pt-Al compounds are stable at least to 1100°C). The coating had an outer region of PtAl<sub>2</sub> (as determined by color) 19 μm thick. No PtAl<sub>3</sub> was observed. Another sample was heated to 660°C for 2 min. The compositional profile of this sample as measured by the electron microprobe technique is shown in Fig. 3. The layers formed are in the sequence of PtAl<sub>4</sub>, PtAl<sub>3</sub>, PtAl<sub>2</sub>, and Pt<sub>2</sub>Al<sub>3</sub>, as would be predicted from the phase diagram.<sup>13</sup> The remaining phases were not observed.

The Pt<sub>2</sub>Al<sub>3</sub> thickness and the absence of PtAl<sub>3</sub> and PtAl<sub>2</sub>, except in particle sintered regions, indicates that the interdiffusion of Al and Pt is quite rapid for

PtAl<sub>3</sub>, PtAl<sub>2</sub>, and Pt<sub>2</sub>Al<sub>3</sub>. The substantial phase formation in 2 min at temperatures as low as 660°C indicates a liquid phase reaction in Al-coated Pt wires. The rapid deposition in aluminization in bulk Pt also indicates a liquid formation.

### C. Aluminization of Pt-Coated IN-738

Samples of IN-738 coated with a variable thickness of Pt were aluminized at 1060°C in argon, using packs containing 3 pct Al. The coatings formed at regions where the Pt layer thickness was about 25, 5, or 0 μm will be used as examples. Micrographs of these samples as deposited, at 0 h and at 3 h of aluminization are shown in Fig. 4. The compositional profiles for the ~25 μm Pt region after 0 and 3 h of aluminization are shown in Fig. 5; those for the ~5 μm Pt region are shown in Fig. 6. The compositional profiles for non-platinum-coated IN-738 shown in Fig. 7 are from a previous study.<sup>10</sup>

For the coating formed at 0 h in the ~25 μm Pt region [Fig. 4(b)], the colors of the two outer regions are comparable to PtAl<sub>2</sub> (yellow) and Pt<sub>2</sub>Al<sub>3</sub> (blue-grey) as observed on aluminized Pt. The PtAl<sub>2</sub> layer is ~22 μm thick. The third region is ~3 μm thick. The high Al and Pt concentrations [Fig. 5(a)] indicate this is primarily a Pt-Al binary phase, most likely PtAl. Microanalysis of the next region shows a sharp

**Table I. Phases Observed in Aluminizing Bulk Platinum**

Phase	Calculated Wt Pct, Pt	Measured Wt Pct Pt*		Measured Wt Pct, Al	Sum	Color of Phase
		A	B			
PtAl <sub>4</sub>	64.4	65.0	59.9	32.3	92.2	White
PtAl <sub>3</sub>	70.6	73.6	72.5	26.0	98.5	Ivory
PtAl <sub>2</sub>	78.3	78.2	76.5	21.3	97.8	Yellow
Pt <sub>2</sub> Al <sub>3</sub>	82.8	82.4	80.5	14.9	95.4	Blue-Grey
PtAl	87.8	87.8	86.0	12.0	98.0	Pink
Pt <sub>3</sub> Al <sub>2</sub>	91.5	91.9	89.7	7.9	97.6	Whitish
Pt <sub>5</sub> Al <sub>3</sub>	92.3					
Pt <sub>2</sub> Al	93.5					
Pt <sub>3</sub> Al	95.6	94.9	91.0	4.9	95.9	White

\*A is the Normalized Value, calculated from the equation:  
 $A = [B / (\text{wt pct Al} + B)] \cdot 100$   
 where B is the weight percent Pt determined by electron microprobe analysis.

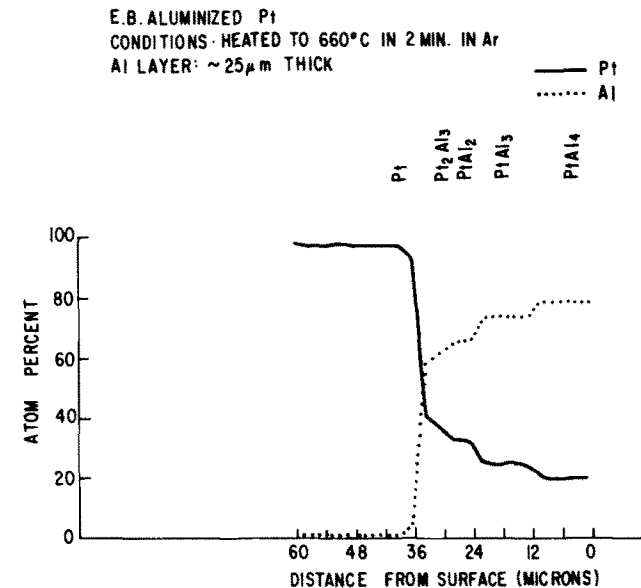


Fig. 3—Compositional profile through E.B. aluminized Pt after a 2 min heat treatment at 660°C in argon.

**Table II. Structures Developed in Aluminizing of Bulk Platinum**

Sample Time at Temp	ΔWt/A, mg/cm <sup>2</sup>	Conditions. 5.8 Wt Pct Al, 1060°C, Argon Layer Thickness, μm							Remarks
		Total	PtAl <sub>3</sub>	PtAl <sub>2</sub>	Pt <sub>2</sub> Al <sub>3</sub>	PtAl	Pt <sub>2</sub> Al	Pt <sub>3</sub> Al	
1) 0 h (sintered particle) 0 h	6.2	68.5 30.4	7.6 0	30.5 0	27.9	2.5	?	NO	See Fig. 2(a)
2) ½ h	7.2	45.7	0	0	33.0	5.1	7.6	Very thin	See Fig. 2(b)
3) 1 h	7.8	48.3	0	0	33.0	6.4	8.9	Very thin	See Fig. 2(c)
4) 3 h	7.8	50.8	0	0	25.4	10.2	15.2	Very thin	See Fig. 2(d)

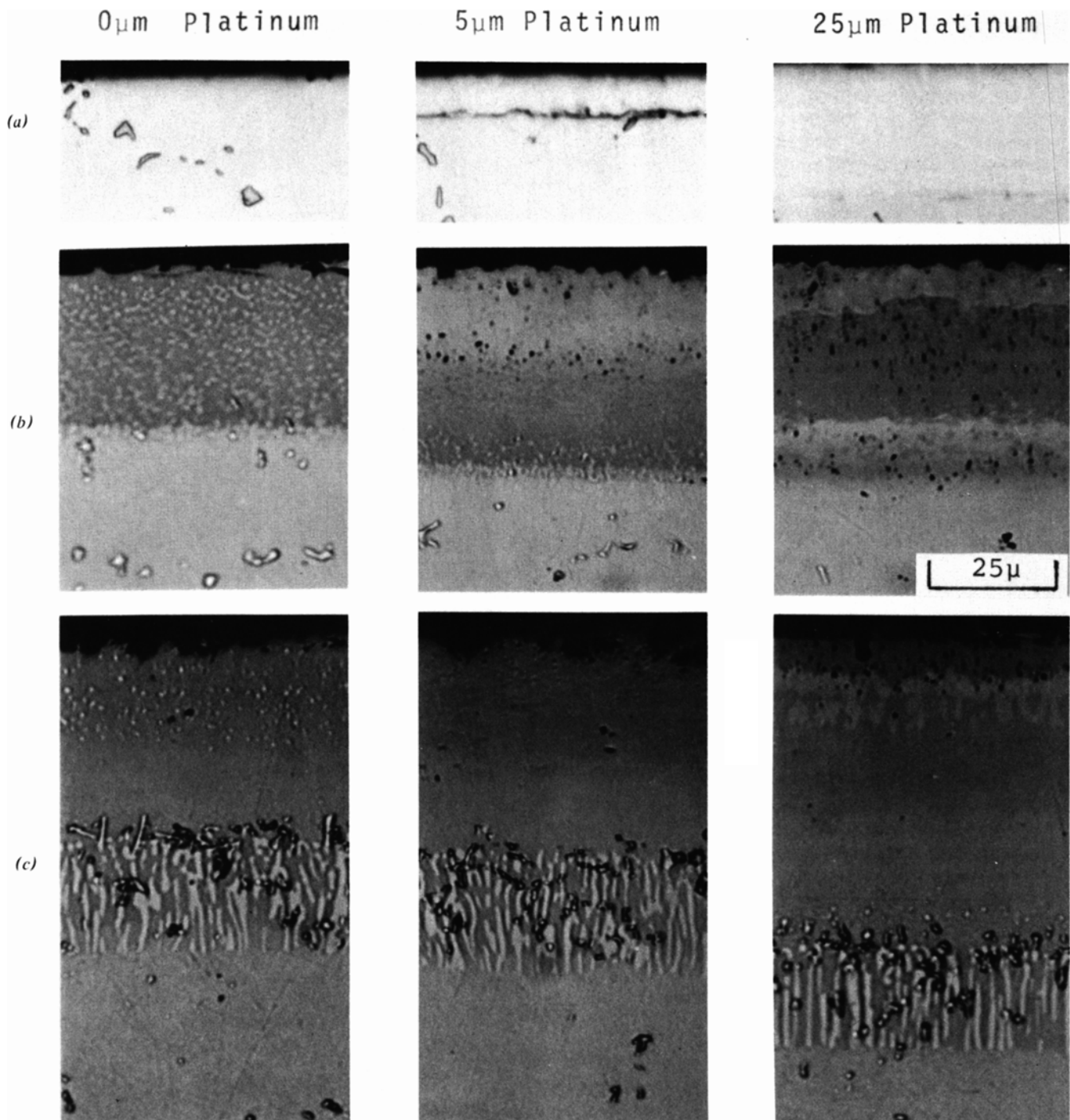


Fig. 4—Microstructures for platinum-coated IN-738 (a) As-deposited, (b) Aluminized for 0 h at 1060°C in a 3 pct Al pack, (c) Aluminized for 3 h at 1060°C in a 3 pct Al pack.

decrease in Al, a sharp increase in Pt, and an increase in Ni, Cr, and the other substrate elements on moving toward the substrate. The structure bordering PtAl appears to be two-phased, and analysis indicates a mixture of PtAl and NiAl. In Fig. 4(b) this region is about 11  $\mu\text{m}$  thick. No further microstructural changes are noted in the sample, although approximately 15  $\mu\text{m}$  of the sample was traversed in microanalysis before compositions returned to the bulk substrate range.

The structures formed at 0 h for aluminized thick-Pt coated IN-738 can be considered as follows. As Al arrives rapidly at the Pt outer surface, a liquid phase

reaction occurs. Solidification occurs rapidly as the liquid dissolves enough of the Pt to form a solid phase. The expected outermost phase is PtAl<sub>3</sub> at 1060°C. However, as was the case for bulk Pt, the Pt coated IN-738 shows PtAl<sub>2</sub> as the outermost composition. Solid-state interdiffusion occurs to produce Pt<sub>2</sub>Al<sub>3</sub> and PtAl, but the other Pt-Al binary phases (Pt<sub>2</sub>Al, Pt<sub>3</sub>Al) are not seen. The phases may be very thin or, because of kinetics of formation, they may be entirely absent. These phases were absent from the aluminized bulk Pt as well.

At zero hour, aluminization is essentially identical

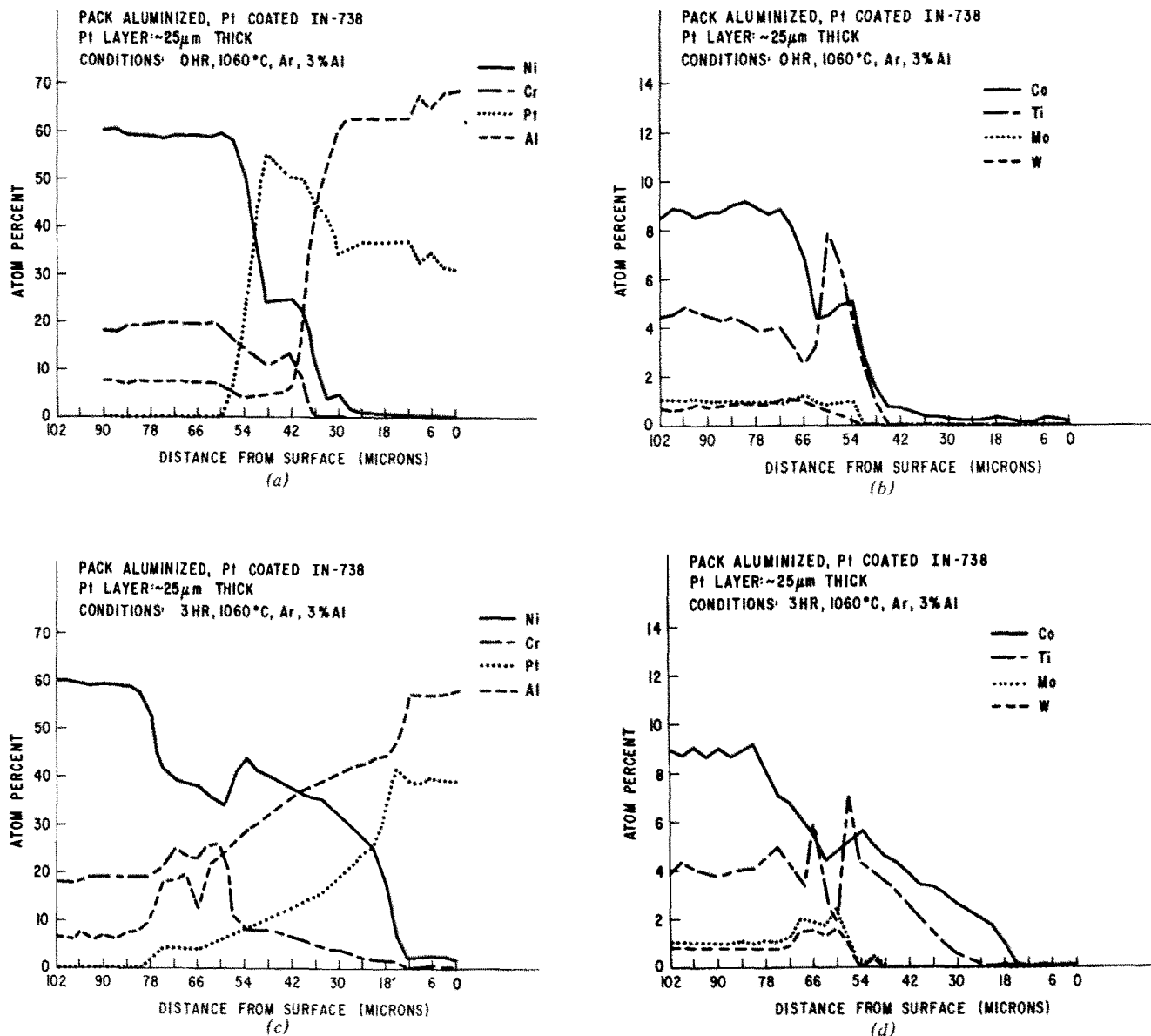


Fig. 5—Compositional profile through pack aluminized Pt-coated (25 μm thick) IN-738 for a 3 pct Al pack at 1060°C, (a) Ni, Cr, Pt, and Al at 0 h, (b) Co, Ti, Mo, and W at 0 hr, (c) Ni, Cr, Pt, and Al at 3 h, and (d) Co, Ti, Mo and W at 3 h.

to aluminization of bulk Pt. At the IN-738/Pt interface, solid-state interdiffusion is occurring throughout the aluminization. The compositional profiles shown in Fig. 5(a) and (b) show this interdiffusion as a decrease in the amount of substrate elements and an increase in the amount of Pt on moving from the substrate to the Pt-rich gamma layer. If the initial Pt layer were much thicker or if much less Al were added, then a 100 pct Pt region, free of interdiffusion effects from either the substrate or the added Al, would be seen. However, sufficient Al has been added at 0 h that the Pt is a noninfinite terminus in both couples: Pt/Al and IN-738/Pt. Microanalysis of the region between the PtAl layer and the Pt-rich gamma layer shows the overlap between the "inward" Al profile and the "outward" substrate element profiles.

To verify the expected behavior when less Al is added, a Pt coated sample of IN-738 was aluminized for 0 h at 1060°C in a lower concentration pack, 1 wt pct Al. Selected points in the aluminized thick Pt re-

gion (25 μm) were chosen for microanalysis. The phases developed were identical with those seen in the 0 h, 3 pct Al pack. However, the maximum concentration of Pt was 73 at pct, compared to 55 at pct Pt in the 3 pct Al pack [Fig. 5(a)].

In the 3 pct Al pack results in Fig. 4, the description of aluminizing of Pt coated IN-738 is quite similar to that of the aluminizing of bare IN-738. After the initial rapid Al deposition and liquid formation and solidification, the Al deposition rate decreases with increasing time. Longer exposures are primarily diffusion heat treatments. The interdiffusion is more complicated because of the presence of the finite-width Pt layer. For example, the 3 h aluminized, thick Pt region can be considered [Fig. 4(c)]. Because of the slow deposition of Al after 0 h and the rapid inward diffusion of Al there is insufficient Al at the surface to maintain PtAl<sub>2</sub>, and Pt<sub>2</sub>Al<sub>3</sub> (8 to 12 μm thick) is seen at the outer surface [Fig. 5(c)]. The substrate elements diffuse outward (with Ni reaching the outer surface in

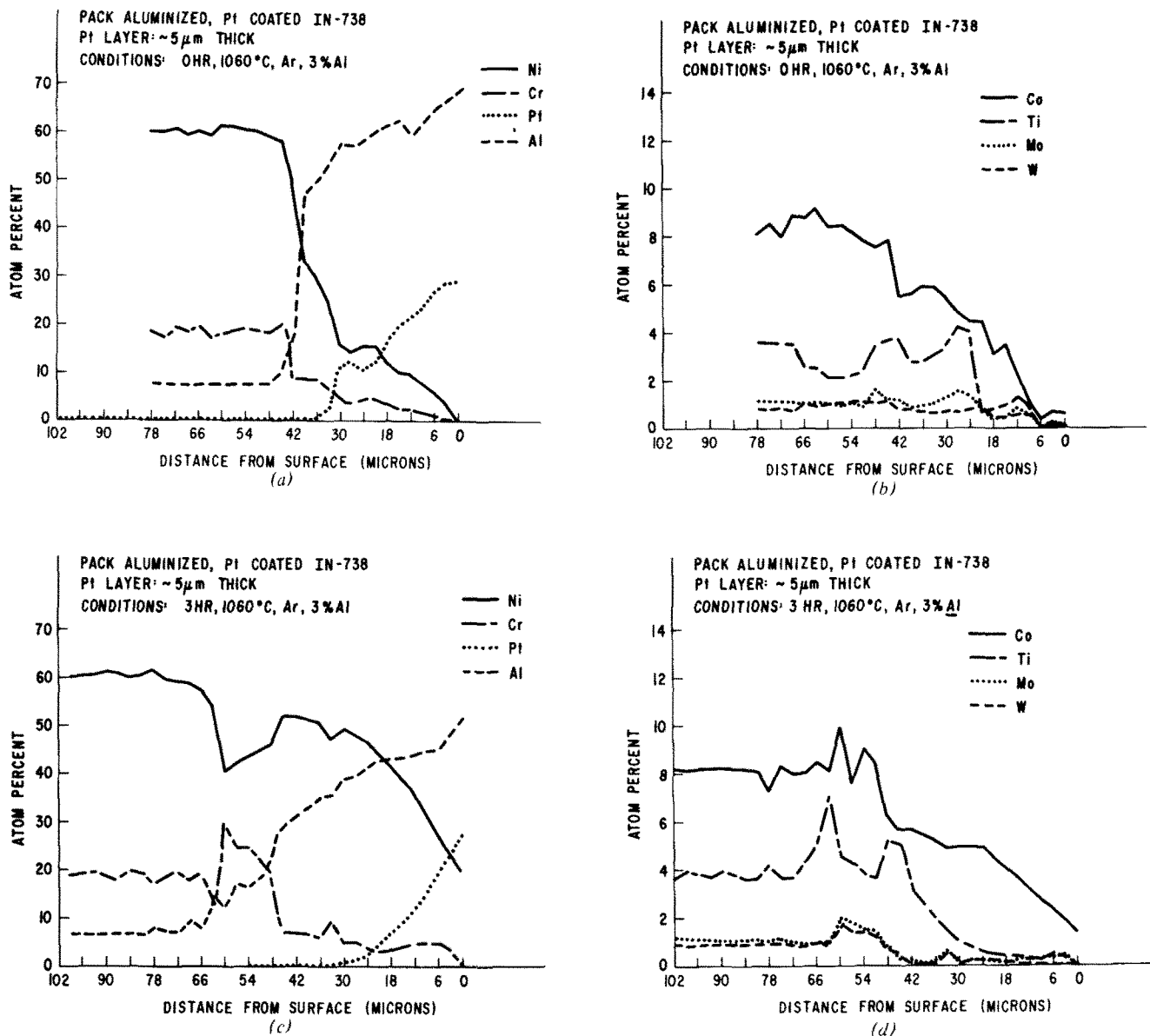


Fig. 6—Compositional profile through pack aluminized Pt-coated ( $5\ \mu\text{m}$  thick) IN-738 for a 3 pct Al pack at  $1060^\circ\text{C}$ ; (a) Ni, Cr, Pt, and Al at 0 h, (b) Co, Ti, Mo, and W at 0 h, (c) Ni, Cr, Pt, and Al at 3 h, and (d) Co, Ti, Mo, and W at 3 h.

concentrations of about 2 pct), and Pt diffuses inward. A  $\sim 3\ \mu\text{m}$ -thick region of PtAl is formed; then  $6\ \mu\text{m}$  of a two-phase mixture of PtAl and NiAl below the PtAl; and then a  $43\ \mu\text{m}$  region where Pt decreases to 8 at pct while Ni increases to 44 at pct. This last  $43\ \mu\text{m}$  region appears to be  $\beta(\text{Ni}, \text{Pt})\text{Al}$ . A peak in refractory elements (Cr, Ti, W, Mo) occurs at  $60\ \mu\text{m}$  from the surface. This corresponds to the approximate location of the original Pt/IN-738 interface.

The peak in refractory elements is seen to coincide with the  $\beta\text{NiAl} + \alpha\text{Cr}$  "finger zone" of Fig. 4(c) that develops in aluminized superalloys. However, no  $\gamma' + \alpha$  zone is observed.

A similar description can be made for the thin-Pt coated IN-738 region (Fig. 4,  $5\ \mu\text{m}$  Pt). For the  $5\ \mu\text{m}$  Pt region, the rapid deposition of  $\sim 25\ \mu\text{m}$  of Al is sufficient to put all of the Pt coating in a two-phase field where one of the phases is liquid at  $1060^\circ\text{C}$ . That is, the  $\sim 25\ \mu\text{m}$  of Al and  $\sim 5\ \mu\text{m}$  of Pt represents a composition which is in the liquid + PtAl<sub>3</sub> phase field for

$1060^\circ\text{C}$  in the Pt-Al binary diagram. The liquid has a solubility for elements in the substrate IN-738, so that dissolution of the substrate will proceed until the liquid composition reaches an all-solid phase field in the quaternary NiCrAlPt diagram used to represent the aluminized Pt and in the ternary approximation of IN-738. The structure shown in Fig. 4(b) and the microanalysis shown in Fig. 6(a) and (b) indicate the state of the aluminized  $5\ \mu\text{m}$  Pt coated IN-738 at 0 h. The very surface of the coating appears to be Ni-free PtAl<sub>2</sub>. The next  $20\ \mu\text{m}$  is Pt<sub>2</sub>Al<sub>3</sub> with  $\sim 0$  Ni at the surface and  $\sim 28$  at pct Ni, Co, Cr, and other substrate elements ( $\sim \text{Ni}_{1.25}\text{Pt}_{0.75}\text{Al}_3$ ) at the inner extreme of the single-phase region. This suggests that Ni<sub>2</sub>Al<sub>3</sub> and Pt<sub>2</sub>Al<sub>3</sub> may be isomorphous. The two pure aluminide phases have the same crystal structure, and the lattice parameters of Ni<sub>2</sub>Al<sub>3</sub> and Pt<sub>2</sub>Al<sub>3</sub> are similar enough to suggest isomorphous behavior. The next  $\sim 18\ \mu\text{m}$  are two-phase, with one phase having the appearance of (Pt, Ni)<sub>2</sub>Al<sub>3</sub>. The second phase is likely to be

$\beta$ NiAl, as indicated by the microanalysis. The last 11  $\mu\text{m}$  before reaching the substrate composition appears to be a transition from  $(\text{Pt,Ni})_2\text{Al}_3 + \beta$  to  $\beta$  and finally to  $\beta + \alpha$  Cr. This is based on the similarity in appearance between this region and the structure noted for aluminized bare IN-738 [Fig. 4(b)].

As before for thick Pt, the 3 h aluminization of the thin-Pt coated IN-738 can be viewed as a diffusion heat treatment of the structure formed at 0 h. The microanalysis [Fig. 6(c) and (d)] shows the outer surface to be an MAI composition (27 at pct Pt, 20 at pct Ni, 2 at pct Co, 51 at pct Al). The outermost 5  $\mu\text{m}$  or so appears to be two-phase (PtAl and  $\beta$ ), but the remainder of the 41  $\mu\text{m}$  outer region appears to be single-phase. The profiles [Fig. 6(c) and (d)] indicate a decrease in Pt and Al and an increase in the substrate elements moving away from the surface. The structural development is  $\beta(\text{Ni,Pt})\text{Al} \rightarrow \beta + \alpha \rightarrow \gamma' + \alpha \rightarrow \gamma + \gamma'$ , similar to the case for aluminizing bare IN-738 [Fig. 4(c) and Fig. 7] at 1060°C.

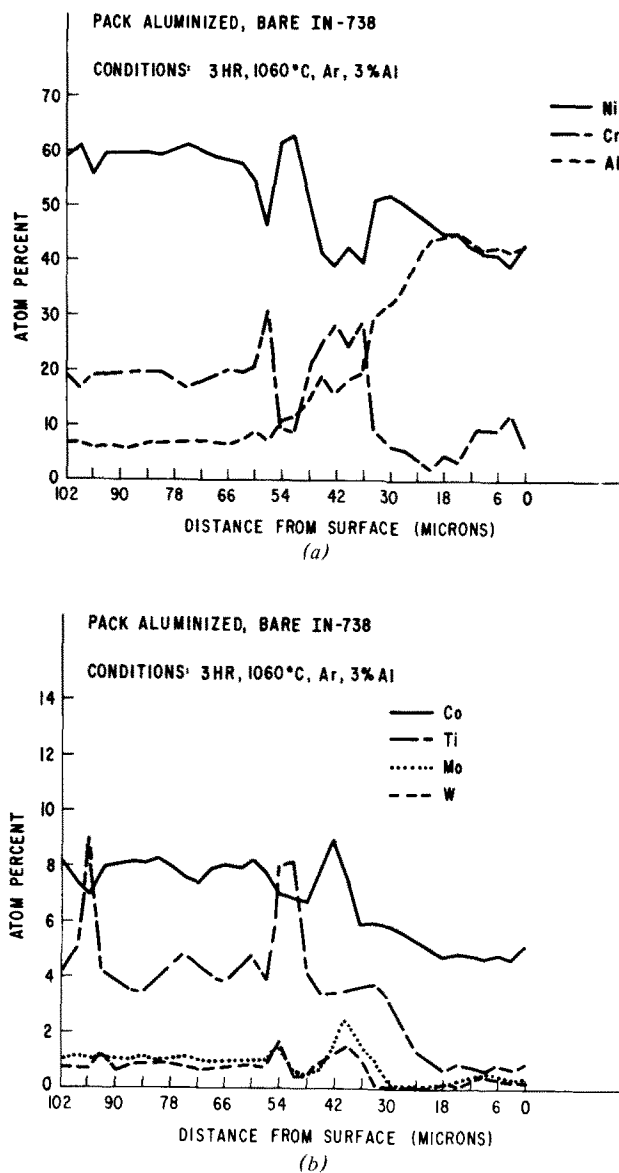


Fig. 7—Compositional profile through pack aluminized IN-738 for a 3 pct Al pack at 1060°C after 3 h, (a) Ni, Cr, and Al, and (b) Co, Ti, Mo, and W.

As was found for aluminizing IN-738,<sup>10</sup> the microstructure developed in aluminizing Pt coated IN-738 follows a general pattern that can be mapped on the appropriate phase diagram. In Fig. 8 is shown a schematic isothermal phase diagram for Ni-Cr-Al-Pt at 1060°C. This diagram is hypothetical but is based on available data and on microstructural observations made in the present study. Possible ternary isothermal sections for NiCrAl and NiCrPt are sketched on the exposed quaternary faces, but the Al-rich phase fields are purely hypothetical. The alloy IN-738 has been approximated as a ternary NiCrAl alloy, 19.5 at pct Cr and 11.8 at pct Al. The heavy dashed lines link the IN-738 substrate with the Pt coating, and the Pt coating to the Al pack source.

For Pt coatings that are thick relative to diffusion distances for a given time-temperature treatment, the system behaves as two unconnected couples: IN-738/Pt and Pt/Al. As the Pt layer becomes thinner relative to diffusion distances, the two couples begin to interact through the common Pt terminus. In Fig. 9 the pyramidal isothermal section has been unfolded to a planar view, with the Al-Cr-Pt ternary omitted. The Al-Cr-Pt diagram is not critical to the explanation, and too little data are available to permit speculation on the appearance of that ternary isothermal section. Approximate diffusion paths, as observed from metallography and microanalysis, have been mapped onto the unfolded quaternary. Each path represents the compositional profile from the coating surface into the substrate. Paths that go through the interior of the quaternary cannot be mapped on the unfolded diagram. However, to a first approximation, all but one of the paths observed in the present study traversed the pyramid along ternary faces or just below the faces.

The path marked 1 is for the case of a Pt coating that is thick relative to diffusion distances. For this case, aluminization occurs only in the Pt, so the initial part of the path is the same as would be seen for aluminization of bulk Pt. The remainder of Path 1 is for diffusion that occurs between bulk Pt and IN-738. Path 2 is for 1060°C aluminization of the ~25  $\mu\text{m}$  thick-Pt coated IN-738 at 0 h. As described earlier, the outer region of this sample is similar to bulk Pt. However, the path departs from that of bulk Pt below the PtAl layer. At this point, the path enters the two-phase PtAl +  $\beta$ NiAl phase field, but it quickly crosses to Pt-rich  $\gamma$  and finally to  $\gamma + \gamma'$  substrate. The diagram is drawn so that a PtAl +  $\gamma$  field exists. It is possible, however, that this field does not exist but is blocked by  $\text{Pt}_2\text{Al} + \beta$  and  $\text{Pt}_3\text{Al} + \beta$  fields. The fact that these fields are not observed in the microstructure described by Path 2 can be explained by the kinetics of formation of  $\text{Pt}_2\text{Al}$  and  $\text{Pt}_3\text{Al}$  in aluminization of bulk Pt.

Path 3 is based on observations of the 3 h aluminization of the thick-Pt coated IN-738. Diffusion of Al inward has eliminated the outer  $\text{PtAl}_2$  region, and diffusion of Pt inward and Ni outward has replaced  $\gamma$  with  $\beta(\text{Ni, Pt})\text{Al}$ . The  $\beta$  phase appears to have a solubility of about 12.5 at pct Pt, with Pt apparently substituting for up to one-fourth of the Ni. For Path 3, a three-dimensional depiction of its position is really more accurate. The path is shown as far as  $\beta$  in the Ni-Al-Pt ternary, and beginning again at  $\beta$  in the Ni-Al-Cr ternary. The path leaves  $\beta$  to form the  $\beta + \alpha$



Cr finger zone, and then goes to the  $\gamma + \gamma'$  substrate. The dashed lines indicate that  $\beta + \alpha$  and  $\gamma + \gamma'$  have a planar interface; that is, dashed lines represent zero distance in the microstructure. The  $\gamma' + \alpha$  phase field, as would be expected for the Ni-Al-Cr ternary isotherm, is not observed. The  $\beta + \alpha$  phase field has been between 5 and 8 at pct Pt [Fig. 5(c)]. This may put the actual path far enough into the quaternary isotherm that a ternary description is no longer valid. In the quaternary isotherm of Fig. 8, as Pt is added to a composition initially in the  $\gamma' + \alpha$  field, the composition may move into a  $\gamma + \gamma' + \alpha$  field, and then to a  $\gamma + \beta + \alpha$  field. Path 3 may pass from  $\beta + \alpha$  to  $\gamma + \gamma'$  at the interface describing passage through the  $\gamma + \beta + \alpha$  field.

Returning to Fig. 9, Path 4 describes the aluminization of thin-Pt coated IN-738 at zero hour. The path begins along the Pt-Al binary but quickly moves into the Ni-Pt-Al ternary isotherm. The Pt content reaches zero in the  $\beta$  phase, so Path 4 is expected to be entirely in the Ni-Cr-Al ternary isotherm from that point on. As is seen for the aluminization of bare IN-738, the path exhibits two finger zones:  $\beta + \alpha$  and  $\gamma' + \alpha$ . Path 5 for the 3 h condition, thin-Pt coated IN-738, begins well into the ternary Ni-Pt-Al. Once again, Pt drops to zero in  $\beta$ , and the remainder of the path duplicates Path 4. Path 6 is the path for 0 Pt; *i.e.*, for aluminization of bare IN-738. For very thin Pt coatings on IN-738, the microstructure would be expected to follow Path 6.

The pattern which emerges from the observed microstructures is complex, but it can be treated with the use of the appropriate diagrams. For the 0 h case, Paths 1, 2, and 4 all start at the same point; *i.e.*, they initially act as though the Pt layer is infinite. A much thinner Pt layer would form an outer  $M_2Al_3$  layer (M-Pt, Ni), and the path would be between Paths 4 and 6. In Fig. 9 the Paths 4 and 6 look very far apart, but if these paths were plotted in Fig. 8, the merging of the two paths would be more evident. With increasing time at temperature, the diffusion paths tend to move in the direction of less Al and less Pt at the surface, as would be expected. Commercial Pt-Al coatings are frequently heat treated at lower temperatures and longer times, but they probably go into service with a coating described by Path 3 or 5. If Al is consumed in service by oxidation or by more rapid inward diffusion than that for Pt diffusion into the substrate, the outer surface composition may again move toward the Pt corner of the quaternary isotherm.

The refractory metals are excluded from the outer surface of the coating of the 25  $\mu\text{m}$  Pt sample and are restricted in the 5  $\mu\text{m}$  Pt sample as compared with nonplatinized IN-738. In the 5  $\mu\text{m}$  Pt region there is not sufficient Pt present to limit the initial liquid formation from involving the substrate, so substrate elements are alloyed with the Pt and Al to form the concentration gradient shown in Fig. 6. Even so, the refractory metal concentration in the outer zone of the 5  $\mu\text{m}$  Pt region is much less than that for nonplatinized IN-738, as can be seen by comparing Fig. 6 with Fig. 7. Herein, at least in part, may reside the reason why platinum aluminized, nickel-base superalloys have such excellent hot-corrosion resistance. Bornstein *et al.*<sup>16</sup> have shown that  $\text{MoO}_3$ , when present above a critical concentration, will accelerate the

$\text{Na}_2\text{SO}_4$  hot corrosion of nickel-base superalloys. If potentially deleterious elements are "buried" beneath the coating, they cannot contribute to accelerated hot corrosion at the surface. Recent studies<sup>17</sup> have indicated Mo is harmful, but it should be noted that other workers<sup>18,19</sup> have shown that Mo, W and Ta can be beneficial to the hot corrosion resistance of Ni-base alloys. Other alternate mechanisms for the benefits of platinum include: a) incorporation in oxide growth stress generation,<sup>20</sup> b) enhanced diffusion of Al in the alloy when Pt is present,<sup>21</sup> and c) improved scale adhesion due to mechanical keying by alloy protrusions into the scale.<sup>22</sup>

A note of caution is offered, based upon observations made in this study. For many of the aluminized Pt coated IN-738 samples examined, there was a strong tendency for partial coating delamination to occur. In some cases, separation occurred at the Pt/IN-738

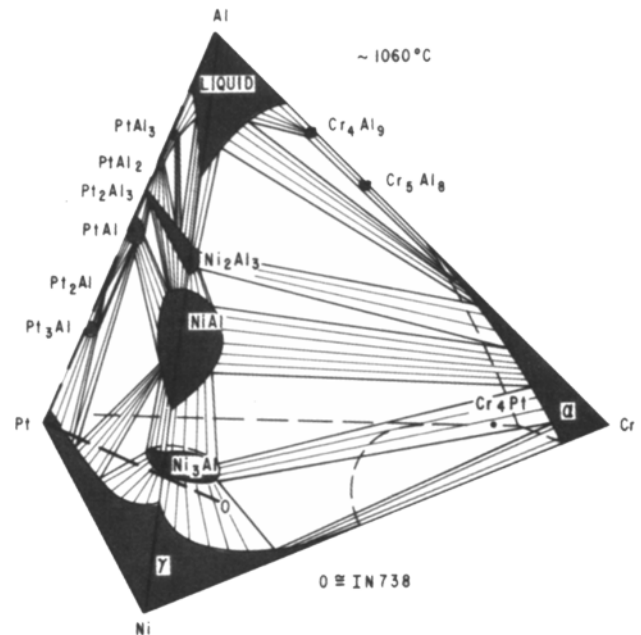


Fig. 8—Schematic 1060°C isothermal section for the Ni-Cr-Al-Pt quaternary phase diagram (hypothetical). The ternary approximation of IN-738 is shown coupled to Pt and the Pt to Al.

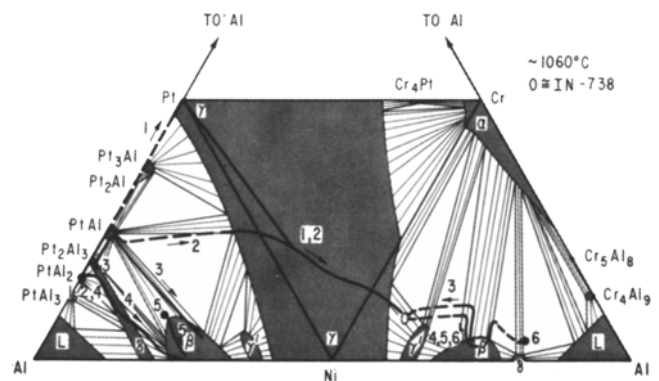
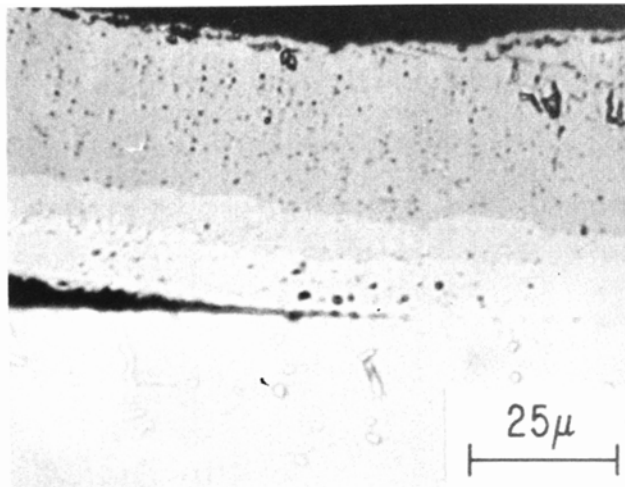
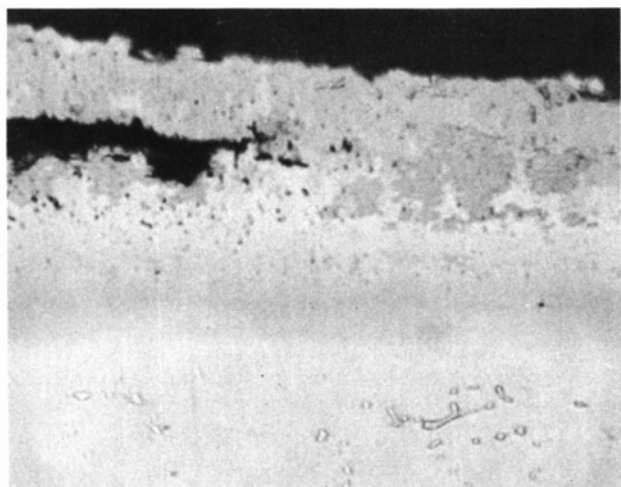
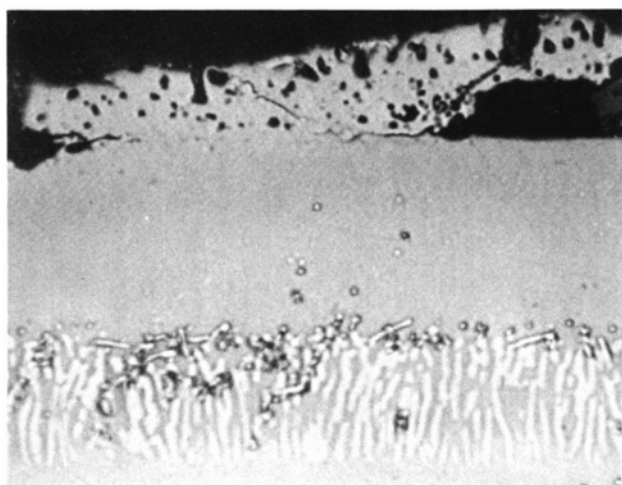


Fig. 9—Schematic diffusion paths for 1060°C aluminization of Pt coated IN-738; (1) aluminization with "infinitely thick" Pt layers, (2) 25  $\mu\text{m}$  thick Pt at 0 h, (3) 25  $\mu\text{m}$  thick Pt at 3 h, (4) 5  $\mu\text{m}$  thick Pt at 0 h, (5) 5  $\mu\text{m}$  thick Pt at 3 h, and (6) non-Pt coated IN-738 at 3 h.



(a)



(b)

Fig. 10—Examples of delamination in coatings formed by pack aluminizing platinized IN-738; (a) Coatings formed at 0 h and (b) Coatings formed at 3 h.

boundary (Fig. 10), indicating failure because of large differences in thermal expansion<sup>23,24</sup> or because of poor initial bond. Another type of delamination (Fig. 10) involved separation along phase boundaries or through phases in the outer Pt, Al-rich regions of the coating. These outer regions are quite brittle. If partial coating delaminations should occur in coated turbine components, it is likely that accelerated localized hot corrosion would result.

#### CONCLUSIONS AND SUMMARY

Based on these data, several observations seem appropriate:

1. As was the case for aluminizing IN-738, a general pattern of microstructures is developed for aluminizing Pt coated IN-738. The pattern can be described in terms of the appropriate phase diagrams.

2. This study has demonstrated that the deposition of a platinum layer onto IN-738 prior to aluminization leads to the reduction, or even elimination of refractory metal elements in the outer region of the final coating. It is suggested that the lowering or elimination of certain refractory elements may account at least in part for the improved hot-corrosion resistance of platinum-aluminized coatings on nickel-base superalloys.

3. There are regions of high Cr and refractory metal concentration in the Pt coated samples [Fig. 5(c) and (d); Fig. 6(c) and (d)], that are similar to those found for non-Pt-coated IN-738 as described in Ref. 3 and as shown in Fig. 7. These regions may form as a result of both solid- and liquid-state diffusion.

4. The Pt remains most concentrated at the surface of the sample after aluminization; these results are similar to those originally reported in Ref. 1. When time is allowed for diffusion, Al can diffuse through the Pt and into the substrate. It seems more appropriate to regard Pt as a diffusion medium rather than as a diffusion barrier for aluminum.

## ACKNOWLEDGMENTS

The microprobe analyses were competently performed by M. D. McConnell, Materials Characterization Branch.

Dr. M. F. Henry performed a critical review of the manuscript, and the authors are indebted to him for suggestions on how to clarify their interpretation of observations.

## REFERENCES

1. A. M. Beltran and D. A. Shores: *The Superalloys*, C. T. Sims and W. C. Hagel, eds., pp. 317-39, John Wiley and Sons, New York, 1972.
2. S. J. Grisaffe: *The Superalloys*, C. T. Sims and W. C. Hagel, eds., pp. 341-70, John Wiley and Sons, New York, 1972.
3. G. Lehnert and H. W. Meinhardt: *D.E.W. Tech. Ber.*, 1971, vol. 11, pp. 236-40.
4. G. Lehnert and H. W. Meinhardt: *Electrodep., Surface Treat.*, 1972-73, vol. 1, pp. 71-76.
5. G. Lehnert and H. W. Meinhardt: *Electrodep. Surface. Treat.*, 1972-73, vol. 1, pp. 189-97.
6. G. Lehnert and H. W. Meinhardt: *Production of Protective Layers on Cobalt-based Alloys*, U. K. Patent No. 1,282,530, 1970.
7. *High-Temperature Oxidation-Resistant Coatings*, ISBN-0-309-01769-6, NAC, NMAB, 1970.
8. N. R. Lindblad: *Oxid. Met.*, 1969, vol. 1, pp. 143-70.
9. G. W. Goward: *J. Metals*, 1970, vol. 22, no. 10, pp. 31-39.
10. J. R. Rairden and M. R. Jackson: General Electric Company, Schenectady, NY, unpublished research, 1974.
11. G. W. Goward, D. H. Boone, and C. S. Giggins: *Trans. ASM*, 1967, vol. 60, pp. 228-41.
12. M. M. P. Janssen and G. D. Rieck: *Trans. TMS-AIME*, 1967, vol. 239, pp. 1372-85.
13. F. A. Shunk: *Constitution of Binary Alloys*, Second Suppl., McGraw-Hill, New York, 1969.
14. M. Hansen: *Constitution of Binary Alloys*, McGraw-Hill, New York, 1958.
15. D. Chatterji, R. C. DeVries, and J. F. Fleischer: *J. Less-Common Met.*, 1972, vol. 42, pp. 187-93.
16. N. S. Bornstein, M. A. DeCrescente, and H. A. Roth: *Met. Trans.*, 1973, vol. 4, pp. 1799-1810.
17. K. R. Peters, D. P. Whittle, and J. Stringer: *Corros. Sci.*, 1976, vol. 16, pp. 791-804.
18. J. W. Schultz and W. R. Hulsizer: *Proc. of the 1975 Gas Turbine Materials in Marine Environment Conference, MCIC, Columbus, Ohio, 1974*, pp. 735-57.
19. H. Morrow III, D. L. Sponseller, and E. Kalns: *Met. Trans.*, 1974, vol. 5, pp. 673-83.
20. J. G. Fountain, F. A. Golightly, F. H. Scott, and G. C. Wood: *Oxid. Met.*, 1976, vol. 10, pp. 341-45.
21. E. J. Felten: *Oxid. Met.*, 1976, vol. 10, pp. 23-28.
22. E. J. Felten and F. S. Pettit: *Oxid. Met.*, 1976, vol. 10, pp. 189-223.
23. *Metals Handbook*, 8th ed., vol. 1, p. 490, American Society for Metals, Metals Park, Ohio, 1961.
24. V. H. Esser and H. Eusterbrock: *Arch. Eisenhuettenw.*, 1941, vol. 14, pp. 341-55.